

Running title: ER organization during tobacco cell division

**Endoplasmic reticulum targeted GFP reveals ER organization in tobacco NT-1 cells  
during cell division**

**Stephanie L. Gupton<sup>a,b 1#</sup>, David A. Collings<sup>a,c\*#</sup>, and Nina Strömngren Allen<sup>a,b</sup>.**

<sup>a</sup>Department of Botany, North Carolina State University, Raleigh, NC 27695 USA.

<sup>b</sup>Marine Biological Laboratories, 7 MBL Street, Woods Hole, MA 02543 USA.

<sup>c</sup>Plant Cell Biology Group, Research School of Biological Sciences,  
The Australian National University, GPO Box 475, Canberra, ACT 2601, Australia.

\* Corresponding author (Fax +61 (2) 6125 4331; E-mail collings@rsbs.anu.edu.au)

# These authors contributed equally to this paper

<sup>1</sup> Current Address: Department of Cell Biology, The Scripps Research Institute, La Jolla,  
CA 92037 USA

E-mail addresses for other authors:

nina\_allen@ncsu.edu

stephg@scripps.edu

**Abstract**

The endoplasmic reticulum (ER) of plant cells undergoes a drastic reorganization during cell division. In tobacco NT-1 cells that stably express a GFP construct targeted to the ER, we have mapped the reorganization of ER that occurs during mitosis and cytokinesis with confocal laser scanning microscopy. During division, the ER and nuclear envelope do not vesiculate. Instead, tubules of ER accumulate around the chromosomes after the nuclear envelope breaks down, with these tubules aligning parallel to the microtubules of the mitotic spindle. In cytokinesis, the phragmoplast is particularly rich in ER, and the transnuclear channels and invaginations present in many interphase cells appear to develop from ER tubules trapped in the developing phragmoplast. Drug studies, using oryzalin and latrunculin to disrupt the microtubules and actin microfilaments respectively, demonstrate that during division, the arrangement of ER is controlled by microtubules and not by actin, which is the reverse of the situation in interphase cells.

*Keywords:* actin microfilaments; cell division; endoplasmic reticulum; green fluorescent protein; microtubules; nuclear envelope; nuclear invaginations

*Abbreviations:* DIC, differential interference contrast; ER, endoplasmic reticulum; GFP, green fluorescent protein

*Supplemental files:*

movie1.avi	accompanies Figure 1 (1.66 MB)
movie2.avi	accompanies Figure 2 (1.78 MB)
movie3.avi	accompanies Figure 3 (0.85 MB)
movie4.avi	accompanies Figure 6 (1.60 MB)

## 1. Introduction

In interphase cells of plants, the endoplasmic reticulum (ER) forms into numerous distinct arrays [16, 39]. These arrays include a comparatively stable, reticulate, cortical network and highly dynamic subcortical ER tubules. These in turn are interconnected and continuous with the nuclear envelope. The presence of these different arrays in living cells was first demonstrated with the carbocyanine dye DIOC<sub>6</sub>(3) and DIC video microscopy [1, 16, 21, 24, 32, 33], and more recently with green fluorescent protein (GFP) targeted to the lumen of the ER [5, 6, 13, 19, 29, 34, 38]. The movement of the motile ER tubules in interphase cells is a microfilament-based process, as actin bundles lie parallel to the ER [1, 5, 25], the motor protein, myosin colocalizes with the ER [25], disruption of the actin cytoskeleton with cytochalasin results in the cessation of ER movement [21]. Actin disruption also prevents the reorganization of ER that precedes cell division in cultured cells [38]. However, the factors responsible for organization of the cortical array, and whether they are cytoskeletal or not, have been more difficult to characterize.

In contrast to the numerous characterizations of ER organization in interphase plant cells, few detailed studies have been published of ER dynamics during plant cell division. This is important, however, for several reasons. First, the ER is continuous with the nuclear envelope during interphase so that proteins localized to the lumen of the ER are also found within the nuclear envelope, and knowing the fate of the ER during mitosis will suggest the localization of luminal proteins [6, 18]. Second, electron micrographs of

dividing plant cells show a close association between tubules of ER that run parallel to the microtubules in both the mitotic spindle [14, 15, 31] and the phragmoplast, the plant specific structure responsible for the formation of the new cell wall in cytokinesis [2]. These results have been confirmed by observations of the accumulation of ER-targeted GFP within the spindle and phragmoplast [29]. It is unknown when in the cell cycle these ER tubules arrive at these regions. Third, phragmoplast formation in plants requires ER and Golgi apparatus-derived vesicles to run along microtubules to the equator of the cell [15, 30] where they consolidate into a sheet that expands outwards as more vesicles fuse, eventually meeting with and fusing with the parent cell wall to complete cell division [35]. Understanding ER dynamics during cell division and their dependence on the cytoskeleton may suggest a mechanism of phragmoplast formation. And finally, some plant nuclei contain deep invaginations and trans-nuclear strands. As these structures are bounded by the nuclear envelope, they are continuous with the ER, but their formation, hypothesized to occur during cell division, remains uncertain [6].

In this study therefore, we have taken advantage of tobacco NT1 and BY-2 cell lines that stably expresses ER-targeted GFP to look at the behavior of ER during cell division, and how the ER interacts with the cytoskeleton. Our data confirm extensive accumulation of ER within the mitotic spindle and phragmoplast, and show that this reorganization of the ER during mitosis is maintained by microtubules, as opposed to the actin cytoskeleton.

## 2. Results

### *2.1. Endoplasmic reticulum organization in interphase cells.*

ER dynamics during interphase and cell division were characterized in tobacco NT-1 cells by visualizing GFP-ER with laser scanning and spinning disk confocal microscopy. In interphase cells, the ER formed three different arrangements, confirming earlier studies that used DIOC<sub>6</sub>(3) to stain membranes [1, 33, 24; our data, not shown], and ER-targeted GFP constructs in cultured tobacco [19, 29, 38] and cell types [5, 6, 13, 34]. First, cortical ER formed polygonal arrays similar to those found in animal cells and other plant cells (Fig. 1A, arrow). The cortical ER exhibited slow movement and intersections of cortical ER were generally three-way. Second, ER tubules extended from the cortical ER into the cytoplasm traversing between vacuoles (Fig. 1B, arrows). This ER was dynamic, and showed rapid cytoplasmic streaming relative to cortical ER, with streaming visible in successive images of a time course (Fig. 1D, arrow). Third, the ER surrounded and was continuous with the nuclear envelope (Fig. 1C,E, arrow). In many interphase cells, penetrations of the nuclear envelope extended into the nucleus forming invaginations and channels that crossed the entirety of the nucleus (Fig. 1E,F; supplemental file movie1.avi) [6]. These channels often showed extensive branching patterns, and could contain internal ER structures suggesting that they contain cytoplasm and ER rather than being a simple infolding of the inner nuclear membrane.

## *2.2. Nuclear envelope / endoplasmic reticulum organization during mitosis and cytokinesis*

Confocal imaging of GFP-ER revealed ER organization during cell division, and showed that vesiculation of the endomembrane system did not occur (Figs. 2, 3; supplemental files movie2.avi and movie3.avi). Prior to nuclear envelope breakdown at the beginning of prophase, but subsequent to chromosome condensation, the nuclear envelope became more brightly labeled (Fig. 2, 0 min; supplemental file movie2.avi) indicating accumulation of ER. As division progressed, the nuclear envelope became oblong and an increasing number of ER protrusions penetrated the nucleus (Fig. 2, 4 and 12 min, arrows) accompanied by a marked increase in the intensity of the ER at the spindle poles. This spindle pole accumulation of ER has previously been reported [29]

As the nuclear envelope dissipated in prophase, ER encompassed the condensed chromatin forming a complicated network of tubules (Fig. 2, 22 min) that eventually was resolved as the metaphase spindle was formed. During metaphase, the ER mimicked the form of the mitotic spindle, and strands of ER were interleaved between metaphase chromosomes that were arrayed at the equator of the cell (Fig. 2, 32 min; Fig. 3, 0 min, arrows). These tubules aligned in the orientation of the spindle, parallel to the presumed orientation of the microtubules. Spindle orientation was determined by observation of chromosomes, either from DIC images, or in optical series where transmitted light images were not collected, from observing the regions in the spindle from which ER was excluded (see also below).

As the chromosomes migrated toward the poles of the cell during anaphase, they continued to be encompassed by tubes of ER, and ER filled the space between the separating sets of chromosomes (Fig. 2, 40 min, arrows; Fig. 3, 3 and 6 min, arrow; supplemental file movie3.avi). As the duplicate pairs of chromosomes were completely segregated, the cell plate and phragmoplast began to form (Fig. 2, 50 min arrow; Fig. 3, 18 min, arrow). Throughout phragmoplast formation, there was a continual increase in the intensity of the GFP-ER to the point of saturation beyond the dynamic range of the detector, indicating rapidly increasing amounts of ER present in the phragmoplast (Fig. 3, 24 to 51 min). Perpendicular strands of ER connected the phragmoplast to the rudimentary daughter nuclei. As the phragmoplast expanded to connect with the cell wall, the nuclear envelopes of the two daughter cells re-formed, and the nucleoli reappeared. Once the phragmoplast and nuclear envelopes had formed, the daughter nuclei shifted away from the new cell wall, and were positioned toward the center of each new cell (data not shown).

### *2.3 ER tubules in the spindle and phragmoplast lie parallel to microtubules*

Our observations of ER tubules in living cells suggested that they lay parallel to spindle and phragmoplast microtubules. We have confirmed this by fixing and immunolabeling the ER-targeted GFP-expressing cells for tubulin (Fig. 4). ER organization in the fixed cells appeared similar to that in living cells throughout the cell



cycle, with extensive subcortical arrays, the nuclear envelope, and nuclear channels and invaginations being visible, suggesting that little ER reorganization occurred during the fixing and immunolabeling procedures. However, we did not observe either the delicate cortical ER array nor the accumulations of ER adjacent to spindle poles. Interphase and prophase cells had distinct cytoplasmic ER and nuclear envelopes with relatively few perinuclear microtubules (Fig. 4A,B). During prophase and prometaphase, ER protrusions formed from the nuclear envelope into the nucleus that contained microtubules (Fig. 4B,C, arrows). In metaphase cells, alignment of ER tubules with the spindle microtubules was apparent (Fig. 4D, arrowheads), with this alignment maintained during anaphase (Fig. 4E, arrowheads), and with the phragmoplast microtubules during telophase (Fig. 4C,F, arrowheads).

#### *2.4. Do interphase nuclear channels form because of lagging chromosomes during cell division?*

Nuclear invaginations and channels were observed in both living (Fig. 1D,E) and fixed interphase cells (Fig. 4A). We previously speculated that nuclear channels might form during cell division [6], and in Figure 3, between 39 and 51 min, nuclear channels in one daughter cell were visible (arrowheads) matching the locations where separating chromosomes lagged in division. As the nuclear envelope reformed around these strands of ER, these internal strands of ER remained within the nucleus, creating the nuclear channels.

### *2.5. Organization of cytoplasmic endoplasmic reticulum during cell division*

As nuclear envelope breakdown progressed, the transvacuolar strands of ER in the cell decreased in number as the ER aggregated around the nuclear region. Although the cytoplasmic ER changed organization, the cortical ER remained in its patterned, fenestrated arrangement beneath the plasma membrane (Fig. 5A, arrow; supplemental file movie4.avi), as seen in interphase. Furthermore, approximately 20 percent of metaphase (Fig. 5A, asterisks) and anaphase cells (Fig. 5B, asterisks) had dense assemblages of ER, visible in both GFP and DIC images, that lay beyond one or both spindle poles, whose location was inferred from DIC images.

### *2.6 Immunofluorescence observations of cytoskeletal disruption and ER organization*

As we were interested in observing the effects of cytoskeletal disruption on ER organization in living cells undergoing division, we used immunofluorescence to assay the effects of drugs that target the cytoskeleton on microtubules and actin microfilaments. Compared to control cells that had extensive arrays of both actin and microtubules (Fig. 6A), 5 min treatments with 5  $\mu$ M latrunculin (Fig. 6B) and 5  $\mu$ M oryzalin (Fig. 6C) caused extensive disruption to the actin and microtubules respectively. These observations are consistent with cytoplasmic streaming slowing immediately, and ceasing

within 12 min following latrunculin treatments (data not shown). Our observations are also consistent with published reports that 5  $\mu\text{M}$  oryzalin disrupts microtubules in cultured tobacco cells [4], and that 1.25  $\mu\text{M}$  latrunculin B causes actin reorganization in tobacco protoplasts [43], with 20  $\mu\text{M}$  latrunculin B causing major actin disruption [12].

### *2.7. Effects of microtubule destabilization on endoplasmic reticulum arrangement*

Oryzalin (5  $\mu\text{M}$ ) caused no obvious changes in ER organization in interphase tobacco NT-1 cells, but significantly changed ER organization in dividing cells (Fig. 7). In prophase cells where the nuclear envelope had broken down, microtubule disruption prevented cells from progressing out of prophase. ER organization also remained in its prophase configuration, characterized by ER encompassing the condensed chromosomes (Fig. 7A). Cells perfused with oryzalin during metaphase also arrested at metaphase, and the tubular strands of the ER network rapidly retracted toward the centrally placed chromosomes (Fig. 7B). Cells perfused with oryzalin after the transition to anaphase exhibited chromosome segregation, but chromosomes did not migrate toward the cell poles. In such cells, the ER lost its tubular appearance (Fig. 7C, 1 min), and the highly prominent ER phragmoplast never formed even after nuclear envelopes reformed around the segregated genetic material, and the nucleoli reappeared in both daughter cells (Fig. 7C, 5 min; compare with Fig. 2, 50 to 60 min and Fig. 3, 18 to 51min). In cells perfused with oryzalin during telophase, once phragmoplast and nuclear envelope formation had already begun, the fluorescence intensity from ER-targeted GFP did not

continue to increase, although nucleoli did reappear within the daughter nuclei (data not shown). These results demonstrate that disruption of microtubules in dividing cells inhibits the normal reorganization of the ER and thus, that ER reorganization must depend upon the microtubule cytoskeleton.

### *2.8. Effects of actin disruption on endoplasmic reticulum arrangement*

In mitotic cells perfused with latrunculin B (5  $\mu$ M) before nuclear envelope breakdown, the processes of cell division and the duration of mitosis, were unaffected and cells continued through the process of cell division, although the cell plate did not form properly between the new daughter nuclei (Fig. 8). Generally, latrunculin did not cause changes to ER organization, although it did cause some cytoplasmic ER to assume a bubble-like vesiculated and disconnected conformation (Fig. 8, 4 min, arrows). Cortical ER remained in its normal configuration, and ER associated with dividing cells was still interspersed in the mitotic spindle (Fig. 8, 0 min, arrows) and prominent in the phragmoplast (Fig. 8, 14 to 26 min, arrowheads). These results demonstrate that changing the organization of actin in dividing cells has little impact on the organization of the ER.

### 3. Discussion

Previous reports of ER during plant cell division have described static images from electron micrographs in which the entirety of ER structure was not visible [14, 15, 17, 20, 31]. Using living cells with GFP targeted to the ER allowed observations of the dynamics of ER. Our data show a reorganization of the ER during cell division, which is directed by microtubules and not actin microfilaments, and which is tubular and not vesicular in nature. These observations are consistent with similar studies conducted in animal cells which demonstrated a close involvement of the ER in cell division, and where nuclear envelope breakdown takes place at the end of prophase/beginning of prometaphase and is preceded by protrusions of the nuclear envelope into the nucleus [40].

#### *3.1. ER organization changes during cell division*

Our observations of GFP-ER in living tobacco NT-1 cells show that the organization of ER changes during cell division. In the initial stages of mitosis, we found that tubules of ER protrude into the nuclear envelope as the chromosomes begin to condense. We confirmed this effect in immunolabeled material, and showed that these ER protrusions contain microtubules. Further, during spindle formation, there is an intense increase in GFP-ER fluorescence at the spindle poles. The nuclear envelope was not observed to "break down" or vesiculate. Rather, it appears that it may be absorbed

into the ER, thereby causing the increase in the intensity of GFP-ER. Were this to be true, the term "nuclear envelope breakdown" would be a misnomer, and would better be termed "nuclear envelope absorption." During metaphase and anaphase, a combination of live cell imaging and immunofluorescence showed that ER tubules lie parallel to the mitotic spindle enmeshing the chromosomes. During cytokinesis, ER accumulates in the phragmoplast where it is involved in the delivery of components to the developing cell plate.

These observations extend electron microscopy analyses that observed tubular ER during plant cell division [14, 15, 31]. Hepler (1980) described ER aggregation at the polar regions of the nucleus following the prometaphase breakdown of the nuclear envelope, and that during metaphase, tubes of ER surround the mitotic apparatus, protrude into its interior and encompass the chromosomes. He also observed aggregations of ER adjacent to the spindle poles of barley cells [14]. Interestingly, Golgi stacks also accumulate around the spindle poles during mitosis [29]. Pickett-Heaps and Northcote (1966) also observed ER tubules interdigitating between chromosomes aligned on the metaphase plate in wheat meristems [31]. We observed similar transitions in living tobacco cells with GFP-ER, including ER aggregates adjacent to the spindle poles of some dividing cells. These studies do, however, stand in contrast to some earlier electron microscopy studies that describe extensive vesiculation of both the nuclear envelope and ER during plant cell division, although they did document similar reorganizations of the ER [20] that may have been caused by the harsh fixations required for electron microscopy.

Our observations of ER during plant cell division match similar observations in various animal cells. Using ER-targeted GFP in insect, echinoderm, and mammalian cells, these studies have shown a general dependence of the organization of the ER in higher eukaryotes on the microtubule cytoskeleton, and that that ER remains continuous during mitosis, as opposed to vesiculating, with the constituents of the nuclear envelope being absorbed by the ER during nuclear envelope breakdown, and then re-emerging from the ER at the end of mitosis [9, 11, 40, 45, 47, 48]. During interphase, the extension of ER tubules occurs as microtubules extend, although depolymerization of microtubules does not disrupt the ER network unless microtubule depolymerization is prolonged [41, 44]. In cell division in sea urchin embryos, similar finger-like indentations of the nuclear envelope occur prior to nuclear envelope break down. Furthermore, microtubules also seem to direct arrangement of ER during cell division. Treatment of mitotic sea urchin embryos with nocodazole, a microtubule depolymerizer, did not prohibit the accumulation of ER at the spindle poles, although the arrangement was irregular and not bipolar [40]. In some mammalian tissue culture cells depolymerization of microtubules induced a distinct loss of organization of the membranous components of the spindles, suggesting that microtubules organize the membrane distribution in some mammalian tissue culture cells. Immunofluorescence studies showed that spindle membranes were associated with microtubules throughout mitosis. These results support the hypothesis that, at least in some cells, ER distribution is maintained by the microtubule cytoskeleton [45]. In *Xenopus* egg extracts, however, the motility of organelles and vesicles along F-actin bundles *in vitro* increases in metaphase bundles compared to interphase, suggesting

that F-actin is active in the dynamics and localization of the ER during cell division [46]. Together, these results suggest that microtubules can organize the distribution of membranes in mitotic cells, and that this organization may vary in different cell types depending on the number of microtubules within the spindle, or other factors such as the role of the actin cytoskeleton and actin-based motors.

### *3.2. The cytoskeleton and endoplasmic reticulum during cell division*

As cells progress from interphase to cell division, the cytoskeletal factors that organize the ER switch from being actin-based to microtubule-based. In interphase cells, actin disruption with latrunculin caused subcortical ER to cease streaming and "bubbles" to form in some of the cytoplasmic ER patterning. Microtubule disruption with oryzalin, however, has little effect on the organization of either the streaming subcortical ER or the polygonal patterning of the cortical ER adjacent to the plasma membrane. These results match previous observations that the dynamic streaming of the subcortical ER occurs through interactions with actin bundles and not microtubules [1, 5, 24, 32], and that ER redistributions prior to cell division are also actin-based [38].

In contrast, ER organization during cell division depends on microtubules and not actin. ER organization is maintained during latrunculin treatments in mitotic cells, consistent with the general lack of actin within the plant mitotic spindle [36]. Our data is also consistent with the functional disruption of the actin cytoskeleton, whether by actin-



or myosin-inhibiting drugs or by profilin microinjections, not delaying mitosis but inhibiting processes in cytokinesis such as the correct formation and alignment of the cell plate [28, 37, 42].

Our data show that the organization of ER around chromosomes during mitosis and cytokinesis depends on microtubules. Not only do both live cell imaging and immunofluorescence show that the ER aligns with microtubules in the spindle and phragmoplast, as previously observed by electron microscopy [14], but microtubule disruption, which blocks cell division, modifies ER organization. Microtubule disruption during metaphase causes the ER to collapse as if the tension suspending the ER had disappeared, while microtubule disruption during anaphase prevents the formation of the ER-rich phragmoplast suggesting that microtubules may be necessary for the localization of this ER. Further, we suggest that microtubules begin directing ER arrangement at nuclear envelope dissipation, and that the ER follows microtubules into the creation of the spindle, continuing through the plane that holds the chromosomes.

Our observations that ER organization during cell division depends in part on microtubules shows that different organelles can behave differently during cell division. For example, the localization of the Golgi apparatus into the so-called Golgi-belt in cytokinetic tobacco BY-2 cells does not depend on either actin or microtubules [29], whereas the redistribution of peroxisomes into a phragmoplast-linked band in dividing onion root tip cells is strictly actin-dependent [8]. Microtubules, however, may be involved in the delivery of ER-derived vesicles to the phragmoplast of cytokinetic

*Arabidopsis* cells through the interaction of a vesicle-localized kinesin, AtPAKRP2, with microtubules [23]. Furthermore, tobacco BY-2 cells contain many different kinesins, and of 15 recently identified kinesins, the majority were shown to be division-specific through northern blot analysis of synchronized cell cultures [27]. There are also upwards of 60 kinesin proteins in the *Arabidopsis* genome, most with unknown functions [22]. Some of these may be the connection between microtubules and ER that occurs in mitosis.

### 3.3. *The formation of nuclear grooves*

Many plant nuclei contain deep grooves, invaginations and channels of cytoplasm that are stable, and which contain actin bundles that support cytoplasmic streaming. We have speculated that such structures might be formed during cell division [6]. Stable and persistent invaginations have also been observed in numerous animal nuclei [10], but their formation has not been described. During cell division in tobacco NT-1 cells, condensed chromosomes are surrounded by ER. In this study, nuclear invaginations formed after cell division in daughter nuclei where chromosomes lagged in the transition from metaphase to anaphase. This suggests that lagging chromosomes may cause an accumulation of leftover ER within the nucleus as the nuclear envelopes for the daughter nuclei reform, and ER is trapped within the nuclei. This observation does not, however, exclude the possibility that nuclear grooves and invaginations can form *de novo* in plant cells during interphase.

## 4. Materials and methods

### 4.1 Plant material

*Nicotiana tabacum* NT-1 suspension culture cells expressing ER-targeted GFP were the kind gift from George Allen and Bill Thompson (North Carolina State University). Protoplasts of the tobacco NT-1 suspension culture line were transformed by electroporation with a pUC-based vector that was derived from the mGFP5 vector developed by Jim Hasseloff [13], and which, like the original vector, contained the cauliflower mosaic virus 35S promoter, signal sequence, GFP construct, HDEL ER retention sequence, and a nopaline synthase terminator. Callus cells were regenerated, and after three weeks, a stable transformant was selected on the basis of high GFP expression. Cells were kept in constant culture with weekly sub-culturing in Murashige and Skoog medium supplemented with 3% sucrose, 1  $\mu\text{g}\cdot\text{ml}^{-1}$  thiamine, 100  $\mu\text{g}\cdot\text{ml}^{-1}$  inositol, 0.2  $\mu\text{g}\cdot\text{ml}^{-1}$  2,4-dichlorophenoxy acetic acid, and 255  $\mu\text{g}\cdot\text{ml}^{-1}$   $\text{KH}_2\text{PO}_4$ , in full darkness at 24°C, with shaking at 125 rpm. For some experiments, we used cells of the closely-related tobacco BY-2 suspension culture line transformed with a similar mGFP5-derived construct [29]. These cells, a kind gift of Andreas Nebenführ (University of Tennessee, Knoxville), were grown under conditions identical to the tobacco NT1 cells. Both cell lines showed similar ER organization during interphase and cell division, and the interphase arrays were similar to published images of tobacco BY-2 cells expressing ER-targeted DsRed [19] and tobacco mesophyll protoplasts expressing ER-targeted GFP [38].

Mitotic cells for the study were obtained from cultures transferred 2 - 4 d prior to the experiment. Synchronization of cells using drug treatment was unnecessary because the actively proliferating young cultures ensured the existence of many mitotic cells.

#### *4.2. Live cell imaging*

Confocal optical sections and time series were collected of cells throughout mitosis and interphase using a Leica TC SP2 confocal laser scanning microscope on either upright or inverted microscopes, with plan-apochromat 40x 1.4 NA oil-immersion and 63x 1.2 NA water-immersion objectives, and with 488-nm excitation. Alternatively, images were collected on an Eclipse TE300 inverted microscope (Nikon, Tokyo, Japan) equipped with an Ultraview spinning-disk confocal system (Perkin Elmer Life Sciences, Boston, MA, USA) with a plan-apochromat 60x 1.2 NA water immersion objective [26] with a plan-apochromat 60x 1.2 NA water immersion objective. GFP was excited at 488 nm, and emission collected through a band pass filter centered at 510 nm. The spinning disk confocal allows high resolution imaging with low excitation to prevent photobleaching and disruption of the cells. Time series of cells progressing through mitosis were recorded with both confocal systems by averaging two images every two or three minutes. Vertical optical sections were collected by averaging two images collected approximately every 0.7  $\mu\text{m}$  through a cell. Images were processed using the Metamorph Image analysis program (Universal Imaging, Downington, PA, USA).

#### *4.3. Live cell specimen preparations*

Cells were imaged in growth media on slides, but for drug treatments involving perfusion of oryzalin or latrunculin, it was necessary to embed the cells in agarose. Untreated cells (200  $\mu$ l) were placed in a well slide and embedded in a thin layer of 1.3% low melting point agarose (type VII, Sigma) in growth media, excess cells and media wicked away, and the media was solidified by placing the cells in the refrigerator for 5 seconds. The well was filled with growth media, and a coverslip placed on top of the well with spacers to allow for perfusion. For microtubule disruption, cells were perfused with 5  $\mu$ M oryzalin in growth media, while for microfilament disruption, perfusion used 5  $\mu$ M latrunculin B. Time series were collected with two images averaged every five seconds for oryzalin treatments, and two images averaged every two minutes for latrunculin treatment. Controls for drug studies were performed with growth media supplemented with 0.5% DMSO.

#### *4.4 Immunofluorescence microscopy*

Cells were washed in cytoskeleton stabilization buffer (CSB; 50 mM Pipes pH 7.2, 2 mM EGTA, 2 mM MgSO<sub>4</sub>) for several minutes will being allowed to settle on slides coated with 0.1% polyethyleneimine. Cells were then fixed in CSB containing 4% formaldehyde, 1% glutaraldehyde, 400 mM maleimidobenzoyl-N-hydroxysuccinimide

ester (MBS; Pierce, Rockford, IL, USA) and 1% dimethylsulfoxide (DMSO) (30 min). After washing in phosphate buffered saline (PBS) (131 mM NaCl, 5.1 mM Na<sub>2</sub>HPO<sub>4</sub>, 1.56 mM KH<sub>2</sub>PO<sub>4</sub> pH 7.2; 2 x 5 min), cells were extracted with methanol at -20°C (20 min) and washed again in PBS. Surprisingly, this methanol extraction did not reduce the fluorescence of the fixed GFP, contrary to previous reports [3] and our own experience [7]. Free aldehyde groups were then reduced with sodium borohydride (5 mg.ml<sup>-1</sup> in PBS) and then washed extensively in PBS. Cell walls were digested (1.0% cellulase and 0.1% pectolyase Y23 (ICN), 1% BSA and 0.3 M mannitol in modified Murashige and Skoog medium; 5 min) and material washed again in PBS (2 x 5 min). After blocking in incubation buffer (PBS containing 1% BSA) (15 min), cells were concurrently immunolabeled (1 h) for actin with rabbit polyclonal anti-maize actin (courtesy of Chris Staiger, Purdue University) (diluted 1/200 in incubation buffer) and mouse monoclonal anti- $\alpha$ -tubulin (Sigma, clone B512) (1/1000). After washing in PBS (4 x 10 min), cells were concurrently incubated in secondary antibodies (1 h), sheep anti-rabbit IgG conjugated to rhodamine (Silenus, Boronia, Victoria Australia) (1/100) and goat anti-mouse IgG coupled to Cy-5 (Jackson, West Grove, PA, USA) (1/200). After washing in PBS (3 x 10 min), DNA was stained with 4',6-diamidino-2-phenylindole (DAPI) (1  $\mu$ g.ml<sup>-1</sup> in PBS; 10 min) and mounted on slides in AF1 anti-fade agent (Citifluor, London, England). For drug studies, oryzalin (5  $\mu$ M) and latrunculin B (5  $\mu$ M) were added to the CSB wash for 5 minutes prior to fixation.

Immunolabelled cells were viewed with the Leica confocal microscope and with a 40X NA1.3 oil-immersion lens. DAPI, GFP, rhodamine and Cy-5 were excited with 351, 488, 543 and 633 nm respectively, with emission windows set to 400-480, 500-530, 550-

600 and 640-760 nm. DAPI and GFP were excited sequentially to eliminate signal cross-talk, with rhodamine and Cy-5 then imaged concurrently.

### **Acknowledgements**

Funding for this project included NASA grant # NAGW-4984 to the North Carolina NSCORT (NASA Specialized Center of Research and Training) (SLG, DAC, NSA), NSF REU Site Grant #0243930 (NSA), a Sigma Xi Grant-in-Aid Award (SLG), and Australian Research Council Discovery Grant no. DP0208806 (DAC). We thank Dana Moxley and Tim Oliver (North Carolina State University) for discussions and cell culturing, George Allen and Bill Thompson for the tobacco NT1 cell line, and Andreas Nebenführ for the tobacco BY-2 cell line. We also thank Edward Salmon and Paul Maddox (UNC - Chapel Hill) for their help with the spinning disk confocal microscope.

## References

1. Allen N.S., Brown D.T., Dynamics of the endoplasmic reticulum in living onion epidermal cells in relation to microtubules, microfilaments and intracellular particle movement. *Cell Motil. Cytoskel.* 10 (1988) 153-163.
2. Bajer A., Fine structure studies on phragmoplast and cell plate formation. *Chromosoma* 24 (1968) 383-417.
3. Billinton N., Knight A.W., Seeing the wood through the trees: a review of techniques for distinguishing green fluorescent protein from endogenous autofluorescence. *Analyt. Biochem.* 291 (2001) 175-197.
4. Binet M.-N., Humbert C., Lecourieux D., Vantard M., Pugin A., Disruption of microtubular cytoskeleton induced by cryptogein, an elicitor of hypersensitive response in tobacco cells. *Plant Physiol.* 125 (2001) 564-572.
5. Boevink P., Oparka K., Santa Cruz S., Martin B., Betteridge A., Hawes C., Stacks on tracks: the plant Golgi apparatus traffics on an actin/ER network. *Plant J.* 15 (1998) 441-447.
6. Collings D.A., Carter C.N., Rink J.C., Scott A.C., Wyatt S.E., Allen N.S., Plant nuclei can contain extensive grooves and invaginations. *Plant Cell* 12 (2000) 2425-2439.
7. Collings D.A., Harper J.D.I., Marc J., Overall R.L., Mullen R.T., Life in the fast lane: actin-based motility of plant peroxisomes. *Can. J. Bot.* 80 (2002) 430-441.
8. Collings D.A., Harper J.D.I., Vaughn K.C., The association of peroxisomes with the developing cell plate in dividing onion root cells depends on actin microfilaments and myosin. *Planta* 218 (2003) 204-216.



9. Ellenberg J., Siggia E.D., Moriera J.E., Smith C.L., Presley J.F., Worman H.J., Lippincott-Schwartz J., Nuclear membrane dynamics and reassembly in living cells: targeting of an inner nuclear membrane protein in interphase and mitosis. *J. Cell Biol.* 138 (1997) 1193-1206.
10. Fricker M., Hollinshead M., White N., Vaux D., Interphase nuclei of many mammalian cell types contain deep, dynamic, tubular membrane-bound invaginations of the nuclear envelope. *J. Cell Biol.* 136 (1997) 531-544.
11. Georgatos S.D., Pyrpassapoulou A., Theodoropoulos P.A., Nuclear envelope breakdown in mammalian cells involves stepwise lamina disassembly and microtubule-driven deformation of the nuclear membrane. *J. Cell Sci.* 110 (1997) 2129-2140.
12. Granger C.L., Cyr R.J., Use of abnormal preprophase bands to decipher division plane determination. *J. Cell Sci.* 114 (2001) 599-607.
13. Haseloff J., Siemering K.R., Prasher D.C., Hodge S., Removal of a cryptic intron and subcellular localization of green fluorescent protein are required to mark transgenic *Arabidopsis* plants brightly. *Proc. Natl. Acad. Sci. USA* 94 (1997) 2122-2127.
14. Hepler P.K., Membrane in the mitotic apparatus of barley cells. *J. Cell Biol.* 86 (1980) 490-499.
15. Hepler P.K., Endoplasmic reticulum in the formation of the cell plate and plasmodesmata. *Protoplasma* 111 (1982) 121-133.
16. Hepler P.K., Palevitz B.A., Lancelle S.A., McCauley M.M., Lichtscheidl I., Cortical endoplasmic reticulum in plants. *J. Cell Sci.* 96 (1990) 355-373.

17. Hepler P.K., Wolniak S.M., Membranes in the mitotic apparatus: their structure and function. *Int. Rev. Cytol.* 90 (1984) 169-238.
18. Herman E.J., Tague B.W., Hoffman L.M., Kjemtrup S.E., Chrispeels M.J., Retention of phytohemagglutinin with carboxyterminal tetrapeptide KDEL in the nuclear envelope and the endoplasmic reticulum. *Planta* 182 (1990) 305-312.
19. Jach G., Binot E., Frings S., Luxa K., Schell J., Use of red fluorescent protein from *Discosoma* sp. (dsRED) as a reporter for plant gene expression. *Plant J.* 28 (2001) 483-491.
20. Jackson W.T., Doyle B.G., Membrane distribution in dividing cells of *Haemanthus*. *J. Cell Biol.* 94 (1982) 637-643.
21. Knebel W., Quader H., Schnepf E., Mobile and immobile endoplasmic reticulum in onion bulb epidermis cells: short- and long-term observations with a confocal laser scanning microscope. *Eur. J. Cell Biol.* 52 (1990) 328-340.
22. Lawrence C.J., Malmberg R.L., Muszynski M.G., Dawe R.K., Maximum likelihood methods reveal conservation of function among closely related kinesin families. *J. Mol. Evol.* 54 (2002) 42-53.
23. Lee Y.-R.J., Giang H.M., Liu B., A novel plant kinesin-related protein specifically associates with the phragmoplast organelles. *Plant Cell* 13 (2001) 2427-2439.
24. Lichtscheidl I.K., Weiss D.G., Visualization of submicroscopic structures in the cytoplasm in *Allium cepa* inner epidermal cells by video-enhanced contrast light microscopy. *Eur. J. Cell Biol.* 46 (1988) 376-382.

25. Liebe S., Quader H., Myosin in onion (*Allium cepa*) bulb scale epidermal cells: involvement in dynamics of organelles and cytoplasmic reticulum. *Physiol. Plant.* 90 (1994) 114-124.
26. Maddox P., Moree B., Canman J.C., Salmon E.D., Spinning disk confocal microscope system for rapid high-resolution, multimode, fluorescence speckle microscopy and green fluorescent protein imaging in living cells. *Meth. Enzymol.* 360 (2003) 597-617.
27. Matsui K., Collings D., Asada T., Identification of a novel plant-specific kinesin-like protein that is highly expressed in interphase tobacco BY-2 cells. *Protoplasma* 215 (2001) 105-115.
28. Molchan T.M., Valster A.H., Hepler P.K., Actomyosin promotes cell plate alignment and late lateral expansion in *Tradescantia* stamen hair cells. *Planta* 214 (2002) 683-693.
29. Nebenführ A., Frohlick J.A., Staehelin L.A., Redistribution of Golgi stacks and other organelles during mitosis and cytokinesis in plant cells. *Plant Physiol.* 124 (2000) 135-151.
30. Nebenführ A., Gallagher L.A., Dunahy T.G., Frohlick J.A., Mazurkiewicz A.M., Meehl J.B., Staehelin L.A., Stop-and-go movements of plant golgi stacks are mediated by the acto-myosin system. *Plant Physiol.* 121 (1999) 1127-1141.
31. Pickett-Heaps J.D., Northcote D.H., Cell division in the formation of the stomatal complex of the young leaves of wheat. *J. Cell Sci.* 1 (1966) 121-128.

32. Quader H., Hofmann A., Schnepf E., Shape and movement of the endoplasmic reticulum in onion bulb epidermal cells: possible involvement of actin. *Eur. J. Cell Biol.* 44 (1987) 17-26.
33. Quader H., Schnepf E., Endoplasmic reticulum and cytoplasmic streaming: fluorescence microscopical observations in adaxial epidermis cells of onion bulb scales. *Protoplasma* 131 (1986) 250-252.
34. Ridge R.W., Uozumi Y., Plazinski J., Hurley U.A., Williamson R.E., Developmental transitions and dynamics of the cortical ER of *Arabidopsis* cells seen with green fluorescent protein. *Plant Cell Physiol.* 40 (1999) 1253-1261.
35. Samuels A.L., Giddings Jr. T.H., Staehelin L.A., Cytokinesis in tobacco BY-2 and root tip cells: new model of cell plate formation in higher plant cells. *J. Cell Biol.* 130 (1995) 1345-1347.
36. Schmit A.-C., Actin during mitosis and cytokinesis. in: Staiger C.J., Baluška F., Volkmann D., Barlow P.W. (Eds.), *Actin: A Dynamic Framework for Multiple Plant Cell Functions*, Kluwer, Dordrecht, (2000), pp 437-456.
37. Schmit A.-C., Lambert A.-M., Plant actin filament and microtubule interactions during anaphase-telophase transition: effects of antagonist drugs. *Biol. Cell* 64 (1988) 309-319.
38. Sheahan M.B., Rose R.J., McCurdy D.W., Organelle inheritance in plant cell division: the actin cytoskeleton is required for unbiased inheritance of chloroplasts, mitochondria and endoplasmic reticulum in dividing protoplasts. *Plant J.* 37 (2004) 379-390.

39. Staehelin L.A., The plant ER: a dynamic organelle composed of a large number of discrete functional domains. *Plant J.* 11 (1997) 1151-1165.
40. Terasaki M., Dynamics of the endoplasmic reticulum and Golgi apparatus during early sea urchin development. *Mol. Biol. Cell* 11 (2000) 897-914.
41. Terasaki M., Chen L.B., Fujiwara K., Microtubules and the endoplasmic reticulum are highly interdependent structures. *J. Cell Biol.* 103 (1986) 1557-1568.
42. Valster A.H., Pierson E.S., Valenta R., Hepler P.K., Emons A.M.C., Probing the plant actin cytoskeleton during cytokinesis and interphase by profilin microinjection. *Plant Cell* 9 (1997) 1815-1824.
43. van Gestel K., Köhler R.H., Verbelen J.-P., Plant mitochondria move on F-actin, but their positioning in the cortical cytoplasm depends on both F-actin and microtubules. *J. Exp. Bot.* 53 (2002) 659-667.
44. Waterman-Storer C.M., Salmon E.D., Endoplasmic reticulum membranes are distributed by microtubules in living cells using three distinct mechanisms. *Curr. Biol.* 8 (1998) 798-806.
45. Waterman-Storer C.M., Sanger J.W., Sanger J.M., Dynamics of organelles in the mitotic spindles of living cells: membranes and microtubule interactions. *Cell Motil. Cytoskel.* 26 (1993) 19-39.
46. Wöllert T., Weiss D.G., Gerdes H.-G., Kuznetsov S.A., Activation of myosin V-based motility and F-actin-dependent network formation of endoplasmic reticulum during mitosis. *J. Cell Biol.* 159 (2002) 571-577.

47. Yang L., Guan T., Gerace L., Integral membrane proteins of the nuclear envelope are dispersed throughout the endoplasmic reticulum during mitosis. *J. Cell Biol.* 137 (1997) 1199-1210.
48. Zaal K.J.M., Smith C.L., Polischuk R.S., Altan N., Cole N.B., Ellenberg J., Hirschberg K., Presley J.F., Roberts T.H., Siggia E., Phair R.D., Lira L.M., Lippincott-Schwartz J., Golgi membranes are absorbed into and reemerge from the ER during mitosis. *Cell* 99 (1999) 589-601.

## Figure Legends

Fig. 1. The organization and dynamics of ER in interphase cells. **(A-D)** Spinning disk confocal optical sections showed polygonal arrays of ER in the outer cortex (**A**, arrow), transvacuolar ER strands that linked the nucleus (n) to the cortex (**B**, arrows), and links between the nuclear envelope and transvacuolar strands (**C**, arrow). **D** Sequential confocal images over 15 seconds showed ER movement in a transvacuolar strand (arrow). **(E-F)** Laser scanning confocal images showing nuclear morphology. **E** A low magnification confocal optical section through a centrally located nucleus (n) with a clear nuclear envelope (arrow). **F** Higher magnification optical sections through only the nucleus, shown at 2  $\mu\text{m}$  intervals from the nuclear surface, reveal an invagination (arrowhead) and a channel that extends across the nucleus and which contains internal structure (arrow). Bar in **A** = 10  $\mu\text{m}$  for **A-C**; bar in **D** = 5  $\mu\text{m}$ ; bar in **E** = 10  $\mu\text{m}$ ; bar in **F** = 5  $\mu\text{m}$ .

Fig. 2. Time-course of confocal fluorescence images showing the changes in ER organization during cell division over 60 minutes, from preprophase through to telophase. In preprophase, ER tubules penetrated the nuclear envelope (4 and 12 min, arrows), rapidly followed by nuclear envelope breakdown at prophase (22 min). Metaphase (32 min) and anaphase (40 min, with arrows indicating ER tubules parallel to the presumed orientation of the microtubule spindle) were followed by a rapid telophase

(42 min onwards) in which the phragmoplast contained increasing amounts of ER. Bar = 5  $\mu\text{m}$  for all images.

Fig. 3. Time-course of changes in ER organization during cell division over 51 minutes, from metaphase through to telophase, showing confocal optical sections and concurrently collected DIC images. In metaphase, strands of ER occurred interleaved between the chromosomes (0 min, arrows). As anaphase commenced, the ER rapidly filled in the space between the separating chromosomes (3 min, arrow). From 18 min onwards, the phragmoplast formed between the new daughter nuclei and laid down the cell plate (arrow in DIC image). The phragmoplast contained ER (arrow in fluorescence and DIC images) in increasing amounts over time, so that eventually the fluorescence signal saturated the detectors of the confocal microscope. Two lagging chromosomes were seen during anaphase (6 min, arrows), and after the nuclear envelope reformed (24 to 33 min), channels of ER crossed the nucleus at the locations of these lagging chromosomes (39 to 51 min, arrowheads). Bar = 10  $\mu\text{m}$  for all images.

Fig. 4. Microtubule and ER organization through the cell cycle. Single confocal optical sections show ER-targeted GFP (top row), immunolabeled microtubules visualized with Cy-5 (middle row) and DAPI-labeled DNA (bottom row). The organization of the chemically-fixed ER was, in general, similar to that seen in living cells. During interphase (A), microtubules remained cortical while ER formed extensive cytoplasmic



and perinuclear arrays. During prophase (**B**) and prometaphase (**C**) as chromatin condensed, increasing numbers of microtubule-containing ER protrusions penetrated the nuclear envelope, and a microtubule spindle developed around the nucleus (arrows). And during metaphase (**D**) and anaphase (**E**), tubules of ER aligned parallel to the microtubules of the spindle (arrowheads), with ER also parallel to the microtubules of the phragmoplast during telophase (**F**) (arrowhead). Images **C** and **F** show the same pair of cells, with the image planes separated by approximately 10  $\mu\text{m}$ . Bar in **F** = 10  $\mu\text{m}$  for all images.

Fig. 5. Dividing cells often show ER aggregates outside the spindle poles. Concurrent confocal fluorescence and DIC images are shown for cells in metaphase (**A**) and anaphase (**B**). **A** During division, the polygonal arrays of cortical ER remained unchanged (arrow), although approximately 20% of dividing cells developed conspicuous assemblages of ER beyond the spindle poles that were visible both by fluorescence and DIC images (asterisks). These aggregations were visible into anaphase (**B**, asterisks). Bar in **A** = 10  $\mu\text{m}$  for all images.

Fig. 6. Drug treatments cause rapid but specific changes to the cytoskeleton. ER-targeted GFP expressing cells were fixed and immunolabeled with Cy-5 for microtubules (top row) and rhodamine for actin microfilaments (bottom row), although ER

preservation in these cells was poor (not shown). Images are maximum projections of confocal optical series through cells. Compared to control cells that contained extensive arrays of both microtubules and microfilaments (**A**), brief (5 - 10 min) treatments with 5  $\mu$ M latrunculin caused disruption only to the microfilaments (**B**). Similar 5 - 10 min treatments with 5  $\mu$ M oryzalin only disrupted the microtubules (**C**). Bar in **C** = 20  $\mu$ m for all images.

Fig. 7. Microtubule disruption with oryzalin during cell division changes the ER organization. Oryzalin (5  $\mu$ M) was perfused into cells in prophase (**A**), metaphase (**B**) and anaphase (**C**). **A** Cells treated with oryzalin in prophase remained trapped at this stage, with ER enmeshed around the chromosomes. **B** In metaphase, oryzalin perfusion caused the collapse of the ER spindle within 1 min. **C** Chromosome separation was inhibited in anaphase cells treated with oryzalin. However, the chromosomes did decondense, and the nuclear envelope reformed within 5 min. A bright, ER-containing phragmoplast never formed between the daughter nuclei in these cells. Bar in **A** = 5  $\mu$ m for all images.

Fig. 8. Latrunculin-mediated actin disruption does not inhibit changes in ER organization during cell division. Confocal sections are shown from a time-series taken over 26 min after application of 5  $\mu$ M latrunculin prior to nuclear envelope breakdown. ER organization looked similar to that of untreated cells. Although some ER “bubbles”

were seen in the cytoplasm (4 min, arrows), the ER still formed arrays that mimicked the mitotic spindle (0 min, arrowheads), and remained prominent within the phragmoplast (14 to 26 mins; arrowheads). Bar = 5  $\mu\text{m}$  for all images.

*Supplemental files:*

[movie1.avi](#) accompanies Figure 1 (1.66 MB)

Optical sectioning through a small part of a cell show a nucleus containing an invagination and a transnuclear channel, both of which contain further ER elements.

Depths from the surface of the nucleus are indicated. Bar = 5  $\mu\text{m}$ .

[movie2.avi](#) accompanies Figure 2 (1.78 MB)

A time course showing changes in ER organization during cell division, over 60 minutes from preprophase through to telophase. In preprophase (0 - 20 min), ER tubules penetrated the nuclear envelope, rapidly followed by nuclear envelope breakdown at prophase (22 - 32 min). During metaphase (32 - 40 min), and a rapid anaphase (42 min), ER tubules lay parallel to the presumed orientation of the spindle microtubules. During telophase (42 min onwards), the phragmoplast contained increasing amounts of ER. As all images in this sequence were collected and processed in a similar manner, the increased intensity of phragmoplast labeling indicates a concentration there of ER. Bar = 5  $\mu\text{m}$ .

[movie3.avi](#) accompanies Figure 3 (0.85 MB)

A time-course showing changes in ER organization during cell division, over 51 minutes from metaphase through to telophase. In metaphase, strands of ER occurred interleaved

between the chromosomes (0 min), but as anaphase commenced (3 min), the ER rapidly filled in the space between the separating chromosomes. Two lagging chromosomes were seen during anaphase (6 min), and after the nuclear envelope reformed (24 - 33 min), channels of ER crossed the nucleus at the locations of these lagging chromosomes. As all images in this sequence were collected and processed in a similar manner, the increased intensity of phragmoplast labeling indicates a concentration there of ER. Bar = 10  $\mu\text{m}$ .

[movie4.avi](#) accompanies Figure 6 (1.60 MB)

Many dividing cells developed conspicuous assemblages of ER beyond the spindle poles.

Depths from the surface of the cell are indicated. Bar = 10  $\mu\text{m}$ .

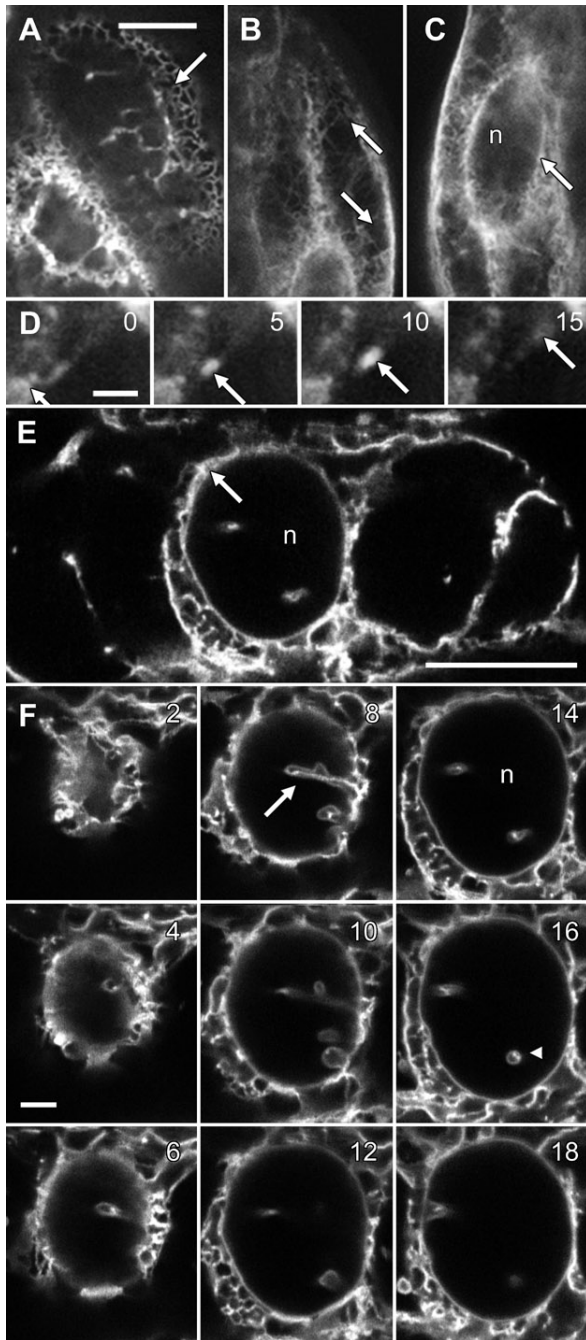


**Figure 1**

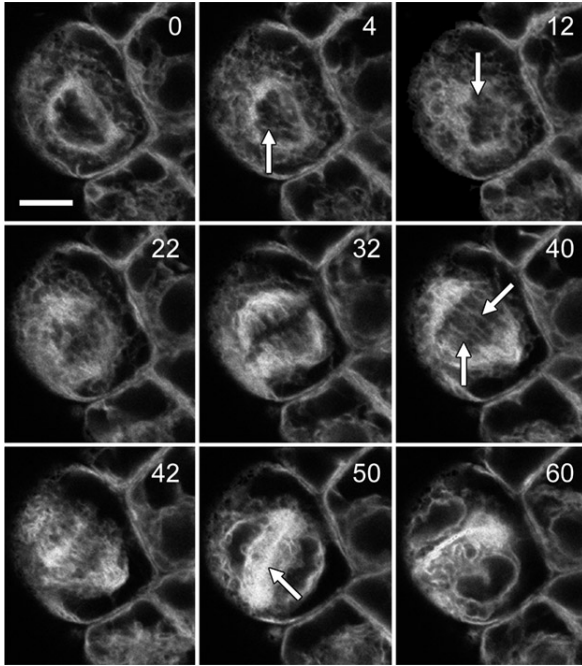


**Figure 2**

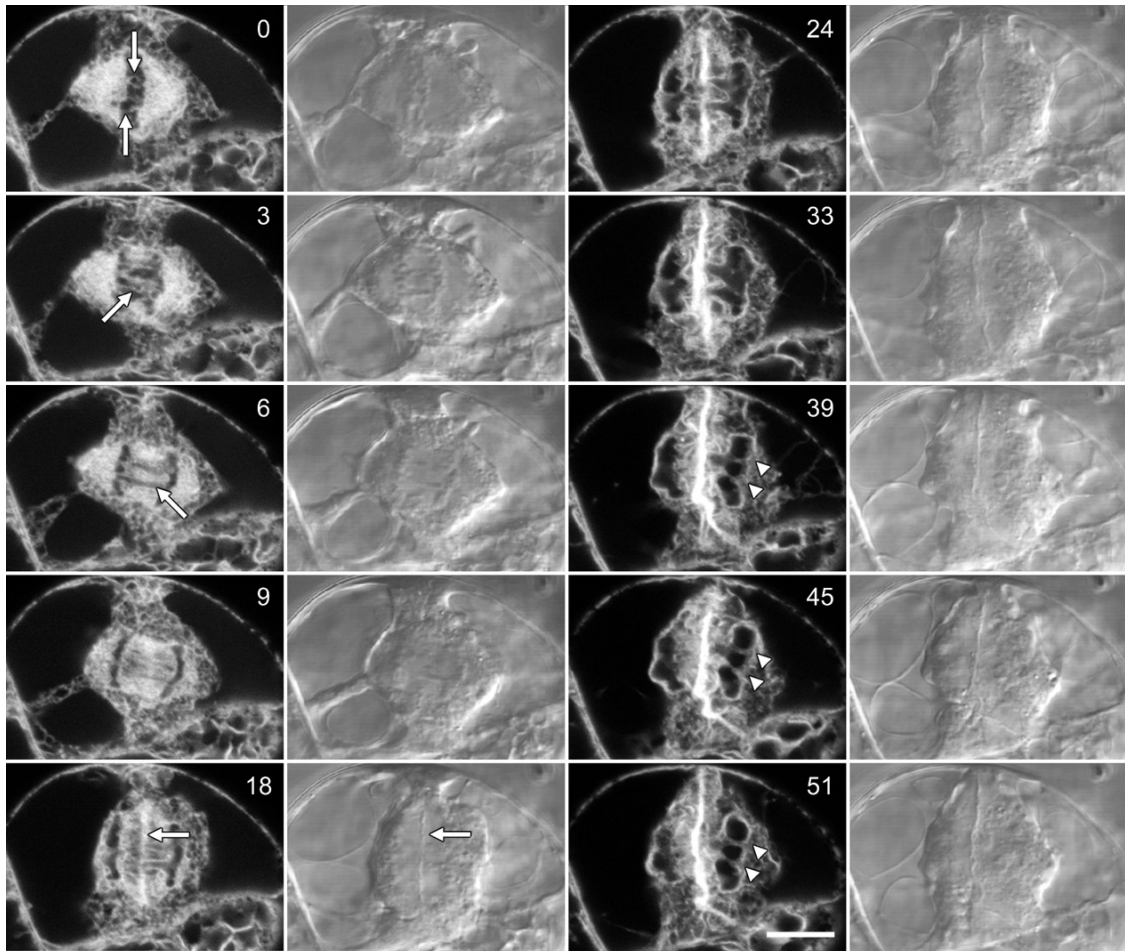


**Figure 3**



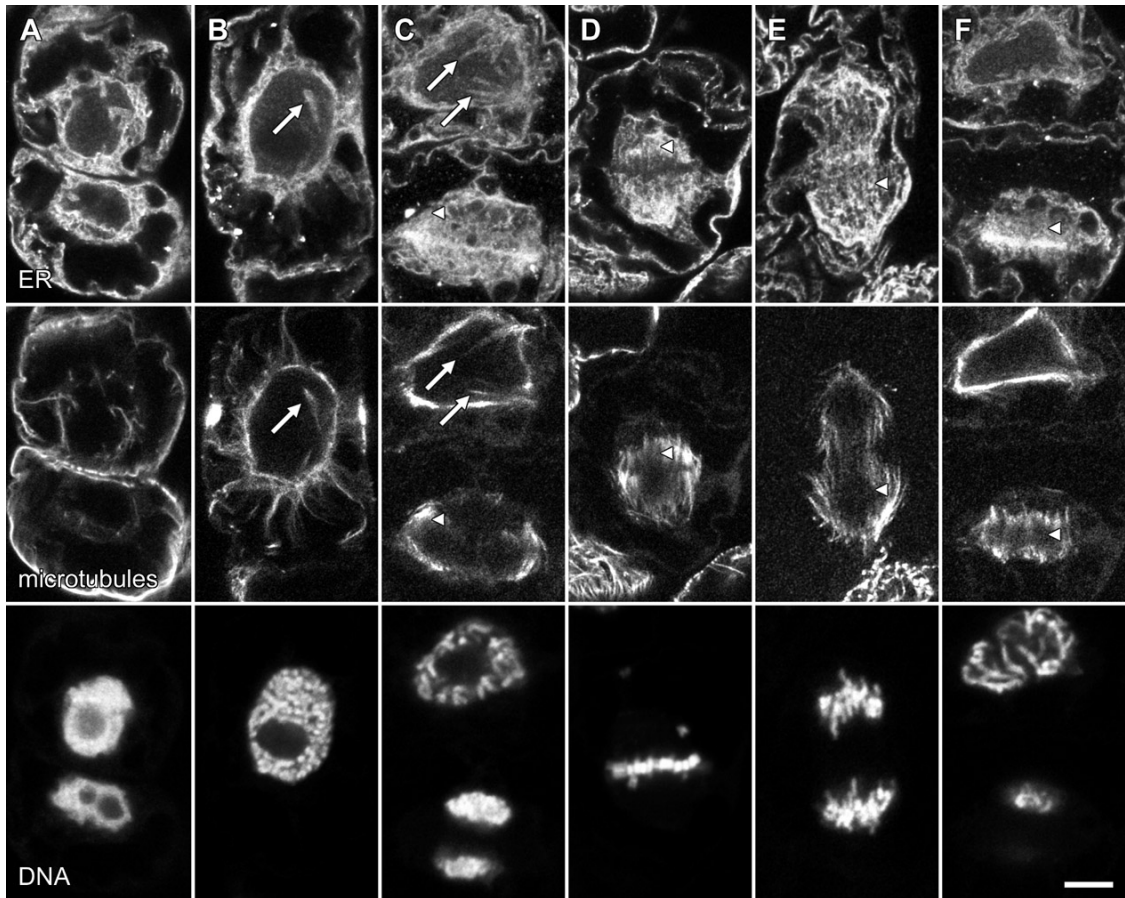


**Figure 4**

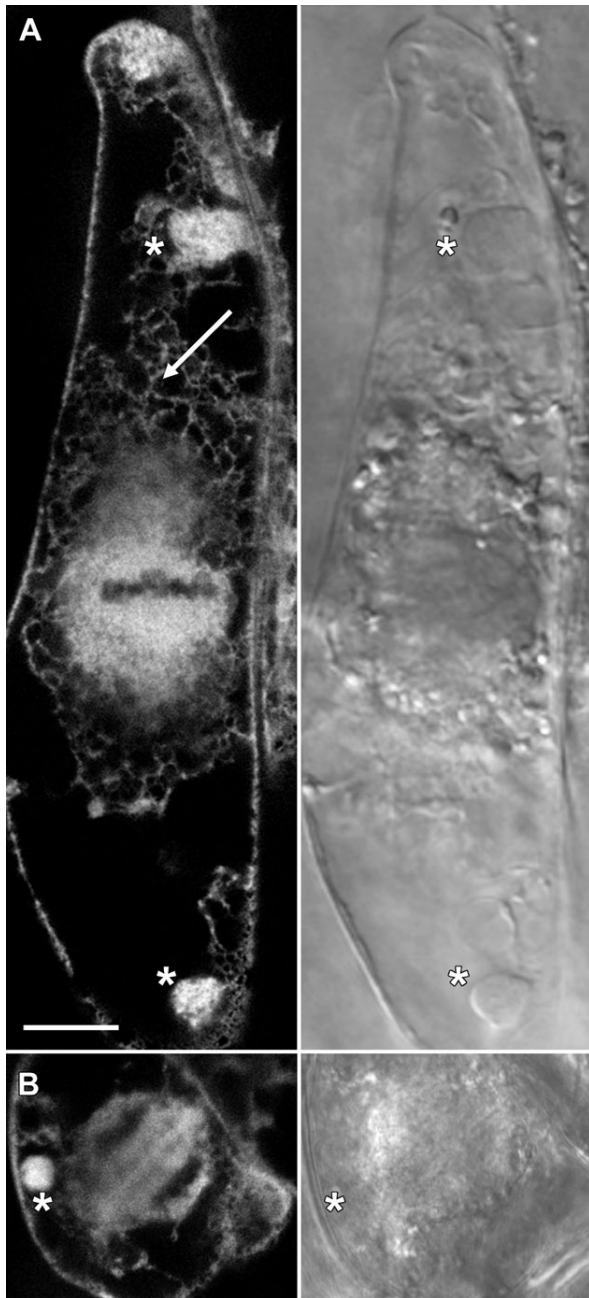


**Figure 5**

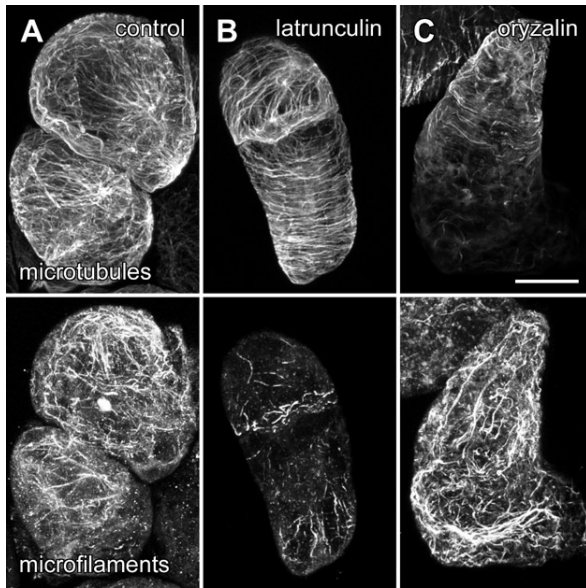


**Figure 6**

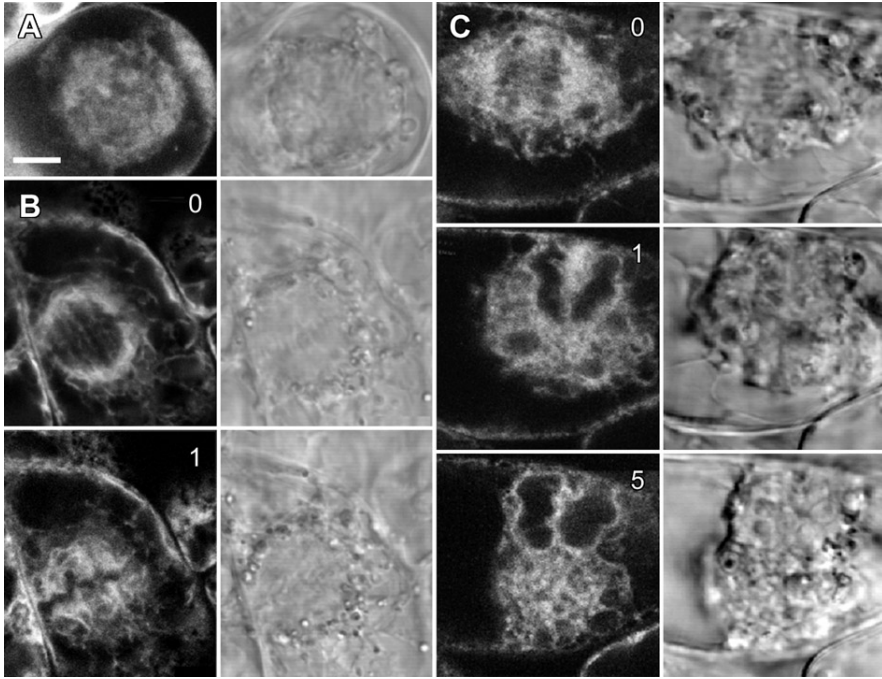


**Figure 7**

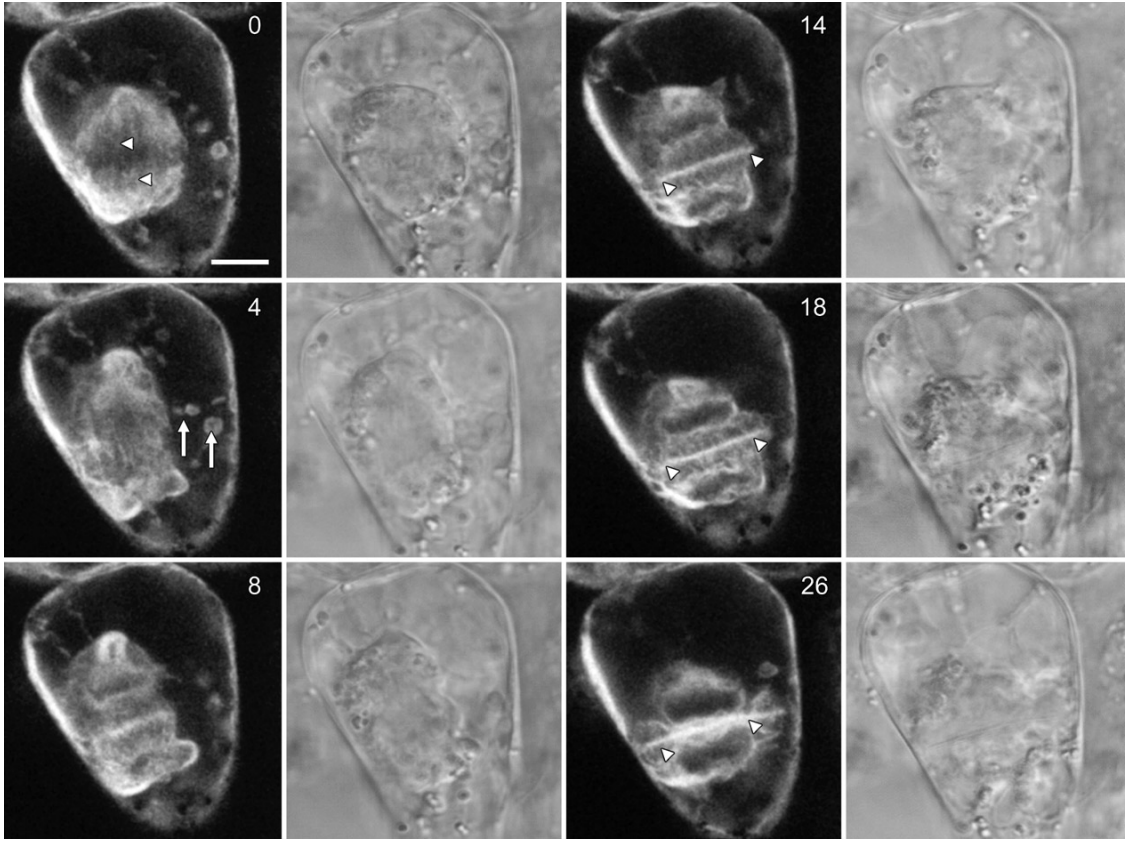


**Figure 8**